Journal of Thermal Analysis and Calorimetry (2019) 136:1147–1152
https://doi.org/10.1007/s10973-018-7823-5

Thermal analysis, crystal structure and magnetic properties of Cr-doped Ni–Mn–Sn high-temperature magnetic shape memory alloys

Medika Kök[1] · S. Burcu Durğun[1] · Ecem Özen[1]

Received: 2 July 2018 / Accepted: 7 October 2018 / Published online: 13 October 2018

Abstract

The superiority of NiMnSn alloy on NiMnGa alloy is far ahead in term of some physical characteristics, and therefore, the development of this alloy group is very important. In this work, $Ni_{50}Mn_{45-x}Sn_5Cr_x$ magnetic shape memory alloys were produced for x = 0, 4, 6, 10 and 12. Thermal analysis was performed on produced alloys in a wide range (200–1000 °C) by using differential scanning calorimetry, thermogravimetric and differential thermal analysis. According to the thermal analysis results, the austenite ↔ martensite transformation temperatures of the NiMnSn alloy decreased with increasing chromium content. Furthermore, the increase in the chromium ratio caused single-phase transformation due to the multiple phase transformation that was observed in the NiMnSn alloy. In addition, the crystal structure and microstructure analyses of the alloys were determined by using X-ray diffraction and scanning electron microscopy–energy-dispersive X-ray spectroscopy. In all cases, martensite and gamma phase were encountered and the gamma phase ratio was found to be increased by chromium addition. The magnetization characteristics were studied by using physical properties measurement systems device, and it was found that the alloys have a considerably small response to magnetic flux.

Keywords Thermal analysis · NiMnSn alloy · Chromium addition · Martensite phase · Gamma phase

Introduction

Shape memory alloys (SMAs) are types of smart materials used in many industrial applications because they have two important features: pseudo-elasticity and shape memory effect. However, brittleness is an inherent disadvantage of these alloys that limited their use [1], and thus, the investigation of finding new alloys or improving their characteristic has become faster [2–5]. SMAs frequently are used in many fields such as automotive, textile, bioengineering, aerospace, composites and microelectromagnetic systems [6, 7]. In general, there are two kinds of microstructural phases in all SMAs which can be specified by binary phase diagrams [8]. The phases are so-called austenite and martensite which are separated by eutectoid temperature. Austenite phase could be observed in the high temperatures, and martensite is the more stable phase in the lower temperatures. These phases in SMAs can be transformed by either mechanical load or temperature stimuli [7, 9].

The alloys that show reversible phase transformation when they exposed to magnetic field are called magnetic shape memory alloys (MSMAs) or ferromagnetic shape memory alloys (FSMAs). MSMAs have brought a different dimension to conventional SMAs, especially those that have attracted attention over the last decade. In MSMAs, the response to temperature and pressure is faster than regular SMAs, and also they have bigger resistance to external influences [1, 10]. The shape of a MSMA can be changed when it is in the martensite phase due to the effect of applying an external magnetic field and the works much faster than the conventional SMA [11]. Underlying these functions lay two fundamental properties: martensite phase transformation and ferromagnetism [12]. FSMAs have become interested due to their remarkable magneto-elastic properties [12–14].

Shape memory effect of a MSMA cannot be controlled by changing temperature like conventional SMAs, but they undergo a structural change due to applying an external magnetic field; thus, they are utilized for magnetic field

✉ Medika Kök
msoglu@firat.edu.tr

[1] Department of Physics, Faculty of Science, Fırat University, Elazig, Turkey

effect actuators [15]. There are lots of MSMAs, but Ni–Mn–Ga alloy is the most studied one. There are many alternatives to this combination, especially the use of Sn instead of Ga, which is preferred in terms of cost reduction, which could be a promising for the future [16]. For this reason, many studies have recently been made on the development of NiMnSn and NiMnSn-based alloys.

In this work, the different amount of chromium addition to NiMnSn alloy has been studied, in order to enhance its shape memory properties. Thus, a high pure chromium powder with various compositional rates was added to the NiMnSn alloy and the thermal properties in a wide temperature range and magnetization features for fabricated alloys have been investigated.

Experimental

First of all, polycrystalline $Ni_{50}Mn_{45-x}Sn_5Cr_x$ (in at.%, x = 0, 4, 6, 10, 12) MSMAs were produced by pelletizing the mixed powders of Ni, Mn, Sn and Cr elements. Then, the pellets were melted by arc melting furnace in a high vacuumed tube and with a non-consumable tungsten electrode. Melting process was repeated several times in the furnace to assure that the alloys have been well homogenized. In addition, the second homogenization process was carried out by keeping all alloys at 900 °C for 24 h. After that, the annealed alloys were quenched in salt-iced water, to avoid no intermediate phases formed during cooling. Then, tiny pieces of each alloy were cut from the ingots to perform differential scanning calorimetry (DSC) with PerkinElmer at a heating and cooling rate of 10 °C min^{-1} and for the temperature range of 200–500 °C. By using results, transformation temperatures including austenite start (A_s), austenite finish (A_f), martensite start (M_s), and martensite finish (M_f) were determined. Also from phase transformations appeared in DSC curves, in each energy exchange, enthalpy change (ΔH) was specified as a thermodynamic parameter. Furthermore, other thermal analysis measurements were taken to determine the phase shift in temperature range of 400–1000 °C by TG/DTA and with the same heating rate DSC measurements. Subsequently, the X-ray diffraction (XRD) measurements were taken for determining crystal structure of the $Ni_{50}Mn_{45}Sn_5$ MSMA with different amount of chromium content. Also, to clarify the microstructural phases and the chemical composition in random positions, the scanning electron microscopy–energy-dispersive X-ray spectrometer (SEM–EDS) was utilized. In addition, chemical mapping measurements were taken to determine the distribution of elements in the alloy. Finally, to determine the magnetic properties of the produced alloys, physical properties measurement systems (PPMS) were handled at room temperature and for magnetic field between − 8 and 8 Tesla.

Results and discussion

Thermal analysis results

Thermal analysis of the $Ni_{50}Mn_{45-x}Sn_5Cr_x$ (in at.%, x = 0, 4, 6, 10, 12) MSMAs in two different kinds of measurements, with DSC in lower temperature and TG/DTA in higher temperature, was performed. The DSC was applied from room temperature to 500 °C with 10 °C min^{-1} of heating–cooling rate, while TG/DTA measurements were taken from 400 °C and 1000 °C with the same heating rate. Figures 1 and 2 illustrate the measurement results of DSC and DTA, respectively, where the peaks and troughs represent phase transformations in each cycle. The quantitative value of electron concentration (e/a), transformation temperatures (A_s, A_f, M_s, M_f) and ΔH is listed in Table 1.

Since none of the samples in the low temperature did not show phase transformation, the DSC curves displayed from 200 to 500 °C. Generally, increasing Cr additional ratio in the $Ni_{50}Mn_{45-x}Sn_5Cr_x$ alloy caused a reduction in the

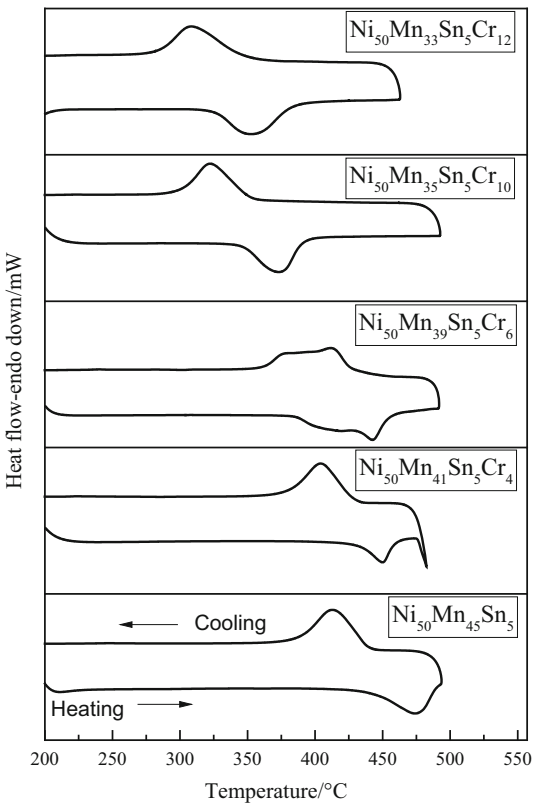

Fig. 1 The heat flux curves of the $Ni_{50}Mn_{45-x}Sn_5Cr_x$ (in at.%, x = 0, 4, 6, 10, 12) alloys were taken at the heating–cooling rate of 10 °C min^{-1} for 200–500 °C

value of both austenite and martensite transformation temperatures. In this study, different compositions of Cr have been added to Ni–Mn–Sn alloy instead of Mn; both of these elements belong to 3D transition metals and their atomic radii are almost the same. Even though both of these elements have nearly the same electronic structure, the chromium element causes a noticeable decrease in the transformation temperatures of the NiMnSn alloy. In addition, Cr element gave rise to vanishing stepped phase transition of the NiMnSn alloy, which is the most significant result of the thermal analysis in this study.

Hu et al. [17] investigated the change in the martensite phase transformation temperature of the NiMnSn alloy by adding iron (Fe) instead of manganese, and consequently, they found that increasing Fe addition led to a falling off in transformation temperature values of the alloy. Likewise, Alexandre Deltell et al. [18] produced $Ni_{50}Mn_{40}Sn_5Co_5$, $Ni_{50}Mn_{37.5}Sn_{7.5}Co_5$ and $Ni_{50}Mn_{35}Sn_{10}Co_5$ (at.%) MSMAs and investigated changes of transformation temperatures of alloys. It was observed that reduction of Mn element in NiMnSn alloy decreased the transformation temperatures of NiMnSn alloy as in our study.

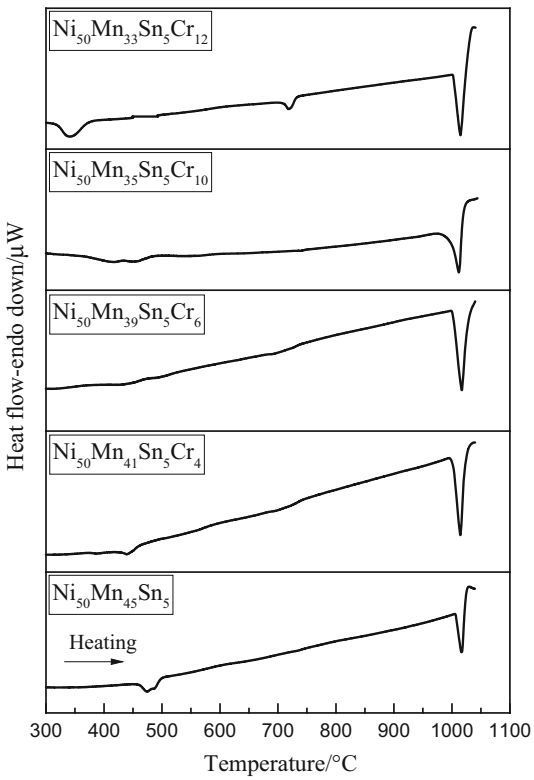

Fig. 2 DTA curves of the $Ni_{50}Mn_{45-x}Sn_5Cr_x$ alloys with x = 0, 4, 6, 10 and 12. The measurements were taken at heating rate of 10 °C min^{-1}

The decrease in martensite transformation temperatures due to doping Cr in NiMnSn alloy could be directly proportional to the electron concentration (*e/a*) values. This reason is consistent with the work of L. Ma and colleagues [13] who studied $Mn_{50}Ni_{50-x}Sn_x$ (x = 0, 2, 4, 6, 8, 9, 10, 10.5, 11) alloys, and they detected that the transformation temperatures have directly affected by electron concentration value. Similarly, Coll et al. [19] got the same result for chromium additive on Mn–Ni–Sn MSMAs. Moreover, Sanchez-Alarcos et al. [20] added Cr to the NiMnIn alloy, and hence, they found that an increase in the rate of Cr caused a decrease in transformation temperatures. Therefore, those results well clarified that Cr element could reduce the transformation temperatures in NiMn-based MSMAs.

TG/DTA measurements were taken for high-temperature thermal analysis. Thus, the technique was used to obtain information about high-temperature phase transformation and determinate oxidation behavior of Ni–Mn–Sn–Cr MSMAs. When the mass gain curves of the produced alloys were examined (Fig. 3), it was observed that the mass gain of the alloys with chromium additive increased instead of manganese. This may due to the fact that the rate of oxidation of chromium is higher than manganese. Similar to DSC, DTA measurements also showed the austenite–martensite phase transformation. These transformation temperatures confirmed with DSC results. The increasing Cr content to 12% at. caused an endothermic reaction appearing in DTA curve around 700 °C. This endothermic reaction is a new solid–solid phase transformation. Commonly, DTA curves showed another endothermic reaction around 1000 °C in both undoped and doped NiMnSn alloys. This is thought to be arising from solid-to-solid phase transformation in the reaction. Similarly, Schlagel et al. [21] found an endothermic reaction in the NiMnSn alloy at the same temperature, and therefore,

Table 1 Electron concentration, phase transformation temperatures and enthalpy changes of the $Ni_{50}Mn_{45-x}Sn_5Cr_x$ SMAs (with at.%, x = 0, 4, 6, 10, 12)

Alloys	*e/a*	A_s/°C	A_f/°C	M_s/°C	M_f/°C	$\Delta H_{heating}$/J g^{-1}	$\Delta H_{cooling}$/J g^{-1}
$Ni_{50}Mn_{45}Sn_5$	8.35	440.3	489.4	439.6	379.0	15.4	− 20.3
$Ni_{50}Mn_{41}Sn_5Cr_4$	8.11	430.9	461.2	427.7	376.4	6.63	− 17.4
$Ni_{50}Mn_{39}Sn_5Cr_6$	7.99	379.4	456.7	428.5	362.2	22.1	− 22.0
$Ni_{50}Mn_{35}Sn_5Cr_{10}$	7.75	346.5	351.6	353.1	294.6	14.6	− 15.7
$Ni_{50}Mn_{33}Sn_5Cr_{12}$	7.63	325.5	384.7	349.9	277.1	16.9	− 18.5

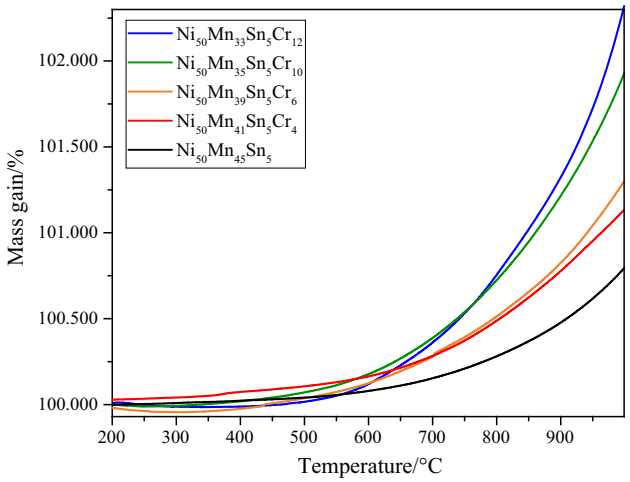

Fig. 3 Mass gain curves of the $Ni_{50}Mn_{45-x}Sn_5Cr_x$ (in at.%, x = 0, 4, 6, 10, 12) alloys for temperature range of 200–1100 °C

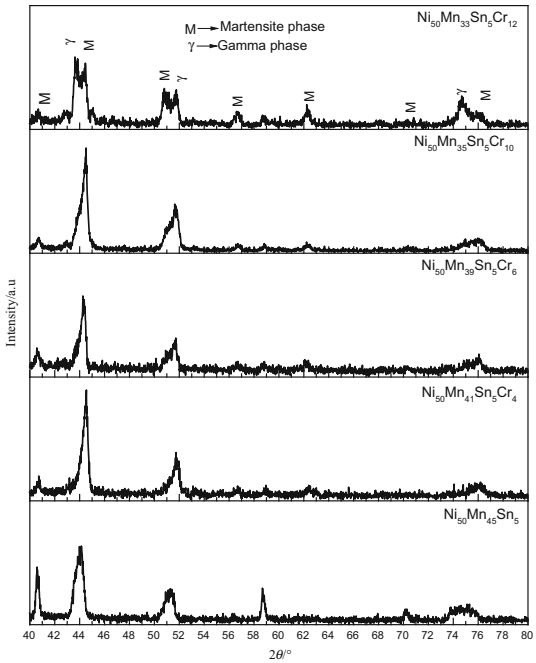

Fig. 4 XRD diffractograms were taken at room temperature for $Ni_{50}Mn_{45-x}Sn_5Cr_x$ alloys (at.%) with x = 0, 4, 6, 10, 12

they defined this reaction as the solidification phase of the alloys.

The XRD measurements were taken at room temperature for $Ni_{50}Mn_{45-x}Sn_5Cr_x$ (in at.%, x = 0, 4, 6, 10, 12) MSMAs, and their patterns are shown in Fig. 4. The peaks have been indexed using the literature [22–25]. In the crystal structure analysis of the alloys, two phases were encountered. The first is tetragonal martensite phase, and the second is the γ (gamma) precipitate phase. The s number and intensity of peaks in the precipitate phase

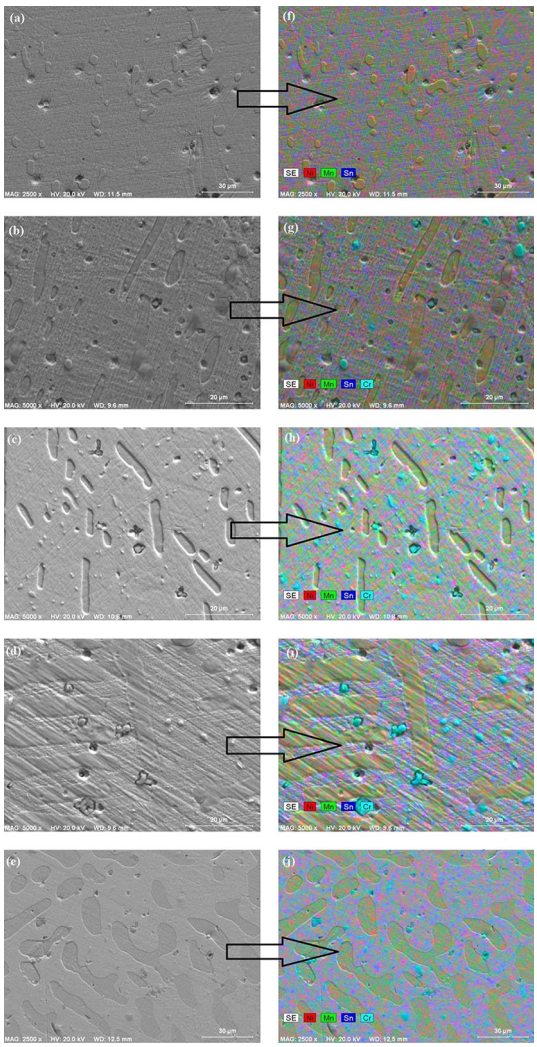

Fig. 5 SEM images of the **a** $Ni_{50}Mn_{45}Sn_5$, **b** $Ni_{50}Mn_{41}Sn_5Cr_4$, **c** $Ni_{50}Mn_{39}Sn_5Cr_6$, **d** $Ni_{50}Mn_{35}Sn_5Cr_{10}$, **e** $Ni_{50}Mn_{33}Sn_5Cr_{12}$ alloys and corresponding chemical mapping for **f** $Ni_{50}Mn_{45}Sn_5$, **g** $Ni_{50}Mn_{41}Sn_5Cr_4$, **h** $Ni_{50}Mn_{39}Sn_5Cr_6$, **i** $Ni_{50}Mn_{35}Sn_5Cr_{10}$, and **j** $Ni_{50}Mn_{33}Sn_5Cr_{12}$ alloys (red → nickel; green → manganese; blue → tin; turquoise → chromium)

increased the reducing chromium content of NiMnSn alloys. The gamma and martensite phase peaks, which are about 44° and 52° in degree, have been split. In the alloy containing the highest chromium element, the peaks belonging to the martensitic matrix phase and the peaks belonging to the secondary phase are clearly separated.

The microimages of SEM for polished and solution-grafted samples are shown in Fig. 5a–d, where matrix in Fig. 5a represents martensite phase in term of plates, and also, bump-like precipitates that distributed as a secondary phase. This precipitation is called gamma phase (γ) which is conformed to corresponding XRD measurement. Chromium contribution changed bumpy precipitation phases to elliptical pit shapes, and it enlarged their shapes too. In

Table 2 EDX results of the $Ni_{50}Mn_{45-x}Sn_5Cr_x$ (in at.%, x = 0, 4, 6, 10, 12) alloys

Alloys	Matrix phase/at.%				Second phase/at.%			
$Ni_{50}Mn_{45-x}Sn_5Cr_x$	Ni	Mn	Sn	Cr	Ni	Mn	Sn	Cr
x = 0	51.34	43.14	5.52	0	57.74	40.60	1.66	0
x = 4	49.98	40.77	5.46	3.79	54.00	39.13	1.60	5.27
x = 6	49.52	38.32	5.55	6.61	53.29	35.79	1.63	9.29
x = 10	51.39	33.69	4.64	10.28	55.47	32.19	1.67	10.67
x = 12	50.85	32.30	5.29	11.55	54.14	31.15	1.63	13.08

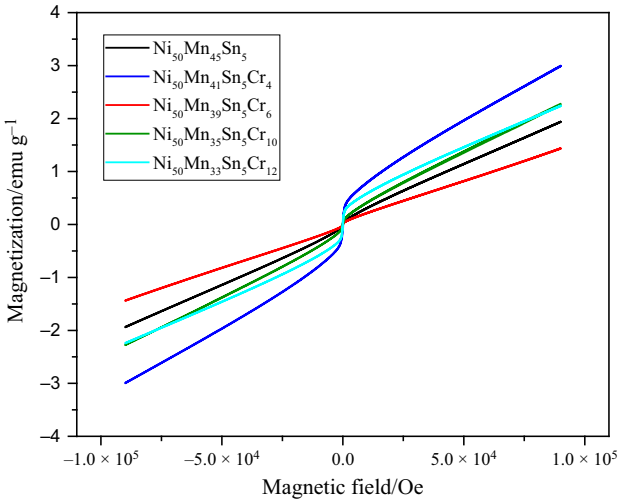

Fig. 6 Magnetization curves of NiMnSnCr alloys at room temperature

addition, chemical analysis (EDX analysis) was performed to determine the rate of composition of different elements in various phases. The atomic percentage of matrix and secondary phases for each alloy is given in Table 2. In matrix of each alloy, the compositional ratio of martensite phase is approximately the same with the predetermined composition. However, EDS result of the secondary phase showed different compositional ratios, and also in all cases, the rate of Sn content stayed constant (about atomic 1.60%). In addition, the rate of Sn element detected in the secondary phase is lower than the matrix phase, while it has higher rate of Cr content compared to the matrix phase. Tan and his colleagues [26] doped iron into NiMnSn alloy, and they have encountered two dominant phases: the matrix and the precipitate phases. In the matrix phase, chemical composition ratio was matched with the defined compositions of the alloy. Even though the amount of Sn in the secondary phase was found to be nearly constant, they concluded that the secondary phase has a gamma precipitate phase. Besides, Wu and colleagues [17] found two phases in the NiMnSnFe alloy group, and therefore, they reported that the Sn ratio in the gamma phase has 1.4% value, which is in good agreement with the result of this study.

Chemical mapping for all specimens is given in Fig. 5f–j, where the Cr-free NiMnSn alloy shows a homogeneous chemical distribution on the basis of colors. For the rest of alloys, Cr homogeneously distributed as sphere-like shapes, which was indicated by turquoise color, and Ni–Mn is the predominant regions. The increase in turquoise color in the map indicates that the number of chromium-rich phase in the alloys increased.

Figure 6 shows the results of magnetization of the NiMnSnCr alloys at room temperature. Magnetization measurements were taken to investigate the effect of Cr addition on the magnetic properties of NiMnSn alloy. It is clearly seen that none of those alloys attained saturation in applying magnetic field of ± 8 Tesla. Also, the magnetization value of all of alloys is in the range of 1.5–3 emu g^{-1}. Aydogdu and colleagues [27] conducted a study on the effect of Sn on magnetization in NiMnSn alloy and found that saturation value decreased by decreasing Sn ratio up to 10%. Hereby, their result gives the tin ratio which is comparably lower than the other groups of NiMnSn alloys, so that is why magnetization values are lower than for all alloys in this study. Also, chromium contribution made a slight increase in magnetization value of the alloy.

Conclusions

In conclusions, the effects of adding Cr on NiMnSn alloy in different ratios were summarized as follows:

- The transformation temperatures of the Ni–Mn–Sn alloy shifted to lower temperatures with addition of chromium and showed a single-step martensite phase transformation while exhibiting a two-step martensite phase transformation.
- It was found that in higher temperatures, chromium addition increased the oxidation rate of the NiMnSn alloy.
- In all cases, XRD patterns and SEM–EDX measurements showed gamma precipitation phase distributed in the matrix of martensite phase, and also, adding

chromium led to an increase in the amount of gamma phase.

- According to the chemical mapping results, the contribution of chromium in the homogenized NiMnSn alloy causes the precipitation phase and the secondary phases to become apparent.
- The magnetization value of NiMnSn and NiMnSnCr alloys IS comparably lower than the same alloys that reported in the literature. The main reason could be the compositional ratio (5 at.%) of Sn content.

Acknowledgements This work has been supported by the Management Unit of the Scientific Research Projects of Firat University (FUBAP) (Project No. FF.17.08). This article is derived from the Master thesis of Şeyda Burcu DURĞUN.

References

1. Zhou Z, Yang L, Li R, Li J, Hu Q, Li J. Martensite transformation, mechanical properties and shape memory effects of Ni–Mn–In–Mg shape memory alloys. Prog Nat Sci Mater. 2018;28(1):60–5.
2. Yang S, Liu Y, Wang C, Lu Y, Wang J, Shi Z, et al. Microstructure and functional properties of two-phase Ni–Mn–Fe–In shape memory alloys with small transformation hysteresis width. J Alloys Compd. 2015;619:498–504.
3. Feng Y, Sui J, Gao Z, Dong G, Cai W. Microstructure, phase transitions and mechanical properties of $Ni_{50}Mn_{34}In_{16-y}$ coy alloys. J Alloys Compd. 2009;476(1–2):935–9.
4. Gao L, Cai W, Liu A, Zhao L. Martensitic transformation and mechanical properties of polycrystalline $Ni_{50}Mn_{29}Ga_{21-x}$Gdx ferromagnetic shape memory alloys. J Alloys Compd. 2006;425(1–2):314–7.
5. Dagdelen F, Aydogdu Y. Transformation behavior in NiTi–20Ta and NiTi–20Nb SMAs. J Therm Anal Calorim. 2018. https://doi.org/10.1007/s10973-018-7635-7.
6. Maji C. Properties of magnetic shape memory alloys in martensitic phase. Curr Sci (00113891). 2017;112(7):1390–01.
7. Heil T. A phase-field computer model of microstructure evolution in a ferromagnetic shape memory alloy. Virginia, USA: Blackburg; 2005.
8. Callister WD Jr. Materials science and engineering: an introduction. New York: Wiley; 2007.
9. Otsuka K, Wayman CM. Shape memory materials. Cambridge: Cambridge University Press; 1999.
10. Malkoc T, Dagdelen F. Production of CoAl and CoAlCr FSMAs and determination of their thermal, microstructure, and magnetic properties. J Therm Anal Calorim. 2018. https://doi.org/10.1007/s10973-018-7508-0.
11. Yang Z, Cong D, Huang L, Nie Z, Sun X, Zhang Q, et al. Large elastocaloric effect in a Ni–Co–Mn–Sn magnetic shape memory alloy. Mater Desgn. 2016;92:932–6.
12. Enkovaara J, Ayuela A, Zayak A, Entel P, Nordström L, Dube M, et al. Magnetically driven shape memory alloys. Mater Sci Eng A. 2004;378(1–2):52–60.
13. Ma L, Wang S, Li Y, Zhen C, Hou D, Wang W et al. Martensitic and magnetic transformation in $Mn_{50}Ni_{50-x}Sn_x$ ferromagnetic shape memory alloys. J Appl Phys. 2012;112(8):083902. https://doi.org/10.1063/1.4758180
14. Sozinov A, Likhachev A, Lanska N, Ullakko K. Giant magnetic-field-induced strain in NiMnGa seven-layered martensitic phase. Appl Phys Lett. 2002;80(10):1746–8.
15. Marioni M, O'Handley R, Allen S, Hall S, Paul D, Richard M, et al. The ferromagnetic shape-memory effect in Ni–Mn–Ga. J Magn Magn Mater. 2005;290:35–41.
16. Czaja P, Maziarz W, Dutkiewicz J. Microstructure evolution and its influence on martensitic transformation in Ni–Mn–Sn alloys. Inżynieria Materiałowa. 2013;34(3):149–52.
17. Wu Z, Liu Z, Yang H, Liu Y, Wu G, Woodward RC. Metallurgical origin of the effect of Fe doping on the martensitic and magnetic transformation behaviours of $Ni_{50}Mn_{40-x}Sn_{10}Fe_x$ magnetic shape memory alloys. Intermetallics. 2011;19(4):445–52.
18. Deltell A, Escoda L, Saurina J, Suñol JJ. Martensitic transformation in Ni–Mn–Sn–Co Heusler alloys. Metals. 2015;5(2):695–705.
19. Coll R, Escoda L, Saurina J, Sánchez-Llamazares JL, Hernando B, Sunol J. Martensitic transformation in Mn–Ni–Sn Heusler alloys. J Therm Anal Calorim. 2010;99(3):905–9.
20. Sanchez-Alarcos V, Recarte V, Perez-Landazabal J, Chapelon J, Rodríguez-Velamazán J. Structural and magnetic properties of Cr-doped Ni–Mn–In metamagnetic shape memory alloys. J Phys D Appl Phys. 2011;44(39):395001.
21. Schlagel D, McCallum R, Lograsso T. Influence of solidification microstructure on the magnetic properties of Ni–Mn–Sn Heusler alloys. J Alloys Compd. 2008;463(1–2):38–46.
22. Xin Y, Li Y, Chai L, Xu H. Shape memory characteristics of dual-phase Ni–Mn–Ga based high temperature shape memory alloys. Scrip Mater. 2007;57(7):599–601.
23. Prasad RVS, Phanikumar G. Amorphous and nano crystalline phase formation in Ni_2MnGa ferromagnetic shape memory alloy synthesized by melt spinning. J Mater Sci. 2009;44(10):2553–9.
24. Ma Y, Jiang C, Li Y, Xu H, Wang C, Liu X. Study of Ni_{50+x}-Mn25Ga_{25-x} (x = 2–11) as high-temperature shape-memory alloys. Acta Mater. 2007;55(5):1533–41.
25. Chen F, Tong Y-X, Tian B, Li L, Zheng Y-F. Martensitic transformation and magnetic properties of Ti-doped NiCoMnSn shape memory alloy. Rare Met. 2014;33(5):511–5.
26. Tan C, Tai Z, Zhang K, Tian X, Cai W. Simultaneous enhancement of magnetic and mechanical properties in Ni–Mn–Sn alloy by Fe doping. Sci Reprt. 2017;7:43387.
27. Aydogdu Y, Turabi A, Aydogdu A, Kok M, Yakinci Z, Karaca H. The effects of boron addition on the magnetic and mechanical properties of NiMnSn shape memory alloys. J Therm Anal Calorim. 2016;126(2):399–406.